

CFD Assessment of COVID-19 Infection Risk in Naturally Ventilated Detached Houses

Chalermwat Tantasavasdi^{1,2,*}, Thawanrat Rianngon¹,
Natthaumporn Inprom^{1,2}

¹Faculty of Architecture and Planning, Thammasat University, Thailand

²Thammasat University Research Unit in Architecture for Sustainable Living and Environment, Thammasat University, Thailand

*Corresponding e-mail: tchalerm@enr.tu.ac.th

Received 2023-10-23; Revised 2024-04-13; Accepted 2024-05-09

ABSTRACT

The airborne nature of COVID-19 dispersion has considerably impacted architectural and ventilation system designs. This research studies the COVID-19 infection risk in typical naturally ventilated detached houses in Thailand. Influencing parameters include the opening size and location of the infected person. Computational Fluid Dynamic was used to simulate the virus spreading in major spaces including the master bedroom, a bedroom and the living room. The Wells-Riley equation was adopted to assess personal infection risk (P_p) and area infection risk (P_a) in 12 case setups. The results reveal that opening size affects more on P_a than P_p . Increasing the opening-to-floor ratio in the range of 0.03 to 0.28 will reduce the P_a and P_p ratios in the range of 0.03 to 0.13 and 0.01 to 0.12, respectively. The location of the source, however, impacts more on P_p than P_a ratios. It varies the trend of the infection risk in the range as high as 0.69 to 0.70 according to other factors including the location of other occupants and the outlet openings.

Keywords: COVID-19 infection risk, Wells-Riley equation, CFD simulation, opening size, location of infected person

INTRODUCTION

Since the turn of the millennium, there have been a number of worldwide outbreaks, especially from respiratory diseases including SARS-CoV-1 in 2003 and MERS-CoV in 2012. However, it is inarguable that the recent SARS-CoV-2 or COVID-19 has created a much bigger global impact than any of its predecessors. From the beginning of the pandemic in 2019, COVID-19 has caused over 770 million infection cases and more than 6.9 million deaths (World Health Organization [WHO], 2023). Thailand has been one of the most affected countries with more than 4.7 million infection cases and over 34,000 deaths (WHO Thailand, 2023). Mobility restriction measures were imposed to prevent the spread (Inthisorn & Puttanapong, 2022). Although COVID-19 was eventually announced as an endemic (Bangkok Post, 2022), its severity level of harm to humanity has already changed people's way of life and created the concept of 'New Normal' in several dimensions.

The pandemic has considerably affected architectural design. Buildings need to better respond to the disease by design innovations (Peters & Halleran, 2021) to create healthy environments (Salama, 2020). Special effort had to be considered in residential buildings because of their impact on people in numerous aspects (Bettaieb & Alsabban, 2021), especially during the lockdown period (Alraouf, 2021). Since the infection of COVID-19 is found to be airborne, the distance between people and ventilation systems is one of the most important factors (Kurnitski, 2020; WHO, 2021). Increasing the ventilation rate generally helps reduce the risk of infection in indoor spaces (Dai & Zhao, 2020; Panraluk & Sreshtaputra, 2020; WHO, 2021). There are guidelines in terms of the minimum rate of air change per hour (ACH) for each type of activity and space, such as a range of 2 to 12 for non-isolated rooms to isolated rooms (Atkinson et al., 2009) and a range of 4 to 6 for homes (Allen & Ibrahim, 2021). Operable windows have been suggested when outdoor conditions allow (Shoen, 2020; American Society of Heating, Refrigerating and Air-Conditioning Engineers [ASHRAE], 2021), encouraging the use of natural ventilation. It was found that, in a natural ventilation mode, the location of the room in relation to the direction of the prevailing wind

significantly affects the ventilation rate (Zhu et al., 2020).

Among two current methods to assess airborne infection probability, the Wells-Riley model has proved to be more effective than the dose-response model (Rayegan et al., 2022). The Wells-Riley equation can be used to initially estimate the overall infection risk of enclosed spaces such as classrooms, office, buses and aircraft cabins (Dai & Zhao, 2020; Kurnitski et al., 2021; O'Donovan & O'Sullivan, 2023; Park et al., 2021). Computational Fluid Dynamics (CFD) has been used to further investigate the airborne dispersion and virus transmission in more details (Mohamadi & Fazeli, 2022). The combination of a CFD study with the Wells-Riley model has been extensively used to calculate the individual infection probability of people in mechanically ventilated spaces, including restaurants (Li et al., 2021), aircraft cabins (Liu et al., 2022) and hospital wards (Li et al., 2023). They found that the location of the infected person and other occupants along with the furniture layout are important influencing factors on infection risk. The study of naturally ventilated spaces, such as those between dormitory units (Dai et al., 2023), also benefits from this method. It reveals that in naturally ventilated spaces where a maximum of 54 ACH can be achieved, which is much higher than that suggested in the guidelines, a high infection risk can still be found, especially in rooms close to the source. Most of the other studies in residential spaces have been relatively limited in the use of tracer gas to assess the infection risk in buildings, such as quarantine hotels (Cheng et al., 2022), dormitories (Zhu et al., 2020) and home quarantine rooms (Cheung et al., 2022) from factors such as opening size and the direction of the prevailing wind in relation to the opening. However, all of the last four aforementioned studies have not included the influences of furniture layout and the location of the infected person and other occupants, which are crucial to compute the infection probability.

This research therefore explores the airborne infection risk from COVID-19 in major spaces of one of the most common residential building types, a detached house in one of the most affected countries, Thailand. We selected a house that accommodates many occupants, thus having a high infection risk as a model in the study. Parameters include opening size and

location of the infected person in relation to other occupants with the consideration of furniture layout. This is because the former directly affects the airflow rate and the latter impacts on the local risk at each spot in a space. We adopted the Wells-Riley model and CFD combination method in this study to calculate the infection probability. The investigation focuses on the use of natural ventilation as it proved to be a better solution for airborne disease prevention while being practical in detached houses in tropical climates (Mediastika et al., 2018) such as those in Thailand (Tantasavasdi et al., 2009).

METHODOLOGY

Identifying a base case and case studies

We selected a base case from a previous study that surveyed countless detached houses around the Bangkok Metropolitan Area (Inprom & Jareemit, 2021). The representative two-storied house (Figure 1) has dimensions of 9.20 x 8.00 m and consists of three bedrooms and three bathrooms. We studied three major functions of the master bedroom, a bedroom and the living room in this research. Both bedrooms are located on the second floor. Each bedroom has openings on two sides and houses two people. The living room is located on the first floor, consisting of a

living area and dining area. It has openings on three sides and has a maximum capacity of seven people.

Most of the typical houses are placed within street grid systems in housing projects. Such alignment makes each house to have its front facing south or north where the local prevailing wind blows from. Therefore, in this study, we specify that the wind derives from the front of the house. In each room, a patient is located as a source of the disease. The location of the source in relation to the wind direction and opening should be an important factor that impacts the infection. For this reason, the source in our study is designated at a location close to the inlet opening (windward side) or close to the outlet opening (leeward side). In the bedrooms, person number 1 and 2 act as the source on the windward side and leeward side, respectively. Consequently, person number 2 and 4 represent the source on the windward side and leeward side, respectively, in the living room. The opening size influences the ventilation rate and therefore represents another significant factor that affects the infection. A sliding window was specified in this study as it is almost the only window type found in typical houses (Inprom & Jareemit, 2021). We selected four window sizes that are most common in typical houses for this study (Table 1). The variation of source location and opening size on the four rooms creates 12 cases in total for this study (Table 2).

Figure 1

Plans of the Base Case: (a) First Floor and (b) Second Floor.

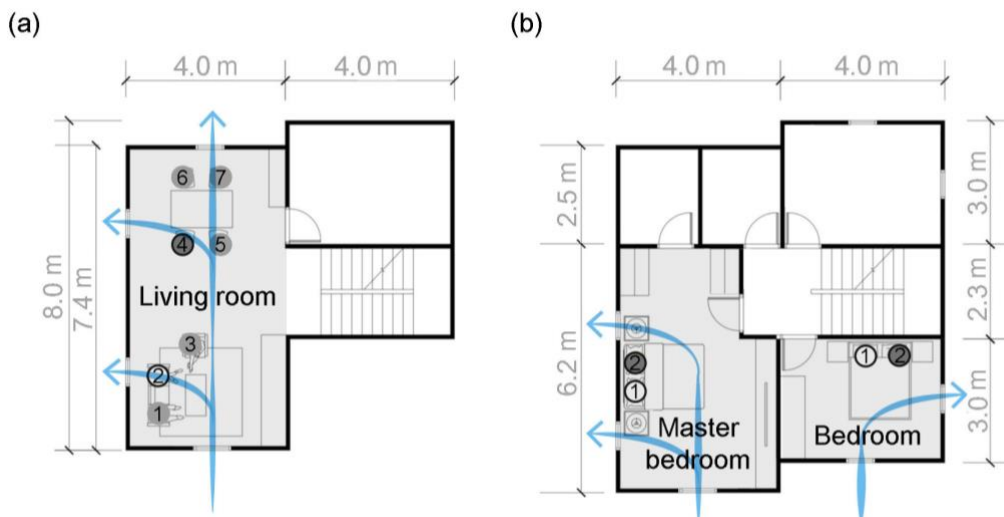


Table 1*Specification of Windows in This Study.*

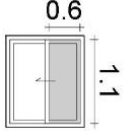
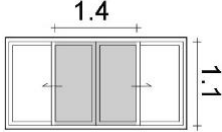
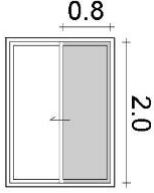
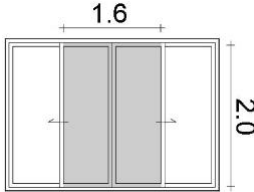
Window number	Window type	Dimensions (m.)	Opening area (m ²)
W1	Single sliding		0.66
W2	Double sliding		1.54
W3	Single sliding		1.60
W4	Double sliding		3.20

Table 2*Details of the 12 Case Studies.*

Room	Opening size	Window combination		Source
		Inlet	Outlet	
Master bedroom	Small	W2	W1 x 2	Windward
	Small	W2	W1 x 2	Leeward
	Large	W4	W2 x 2	Windward
	Large	W4	W2 x 2	Leeward
Bedroom	Small	W2	W1	Windward
	Small	W2	W1	Leeward
	Large	W2	W2	Windward
	Large	W2	W2	Leeward
Living room	Small	W3	W1 x 3	Windward
	Small	W3	W1 x 3	Leeward
	Large	W4	W2 x 2 + W4	Windward
	Large	W4	W2 x 2 + W4	Leeward

CFD simulation setups and validation

To assess the COVID-19 infection risk in this study, a CFD program, PHOENICS (Concentration, Heat and Momentum Limited [CHAM], 2021) was used to simulate the airflow in and around the building. In each case, the house was modelled as a single house located in the middle of the domain with no surroundings. It has substantial distances from the boundaries of the domain to fully capture the development of the airflow (Figure 2). The distances were considered as proportional to the building's height (H): 6H at the front and top, 3H at the sides and 10H at the back of the building. The prevailing wind profile was modelled as several staggering inlets with different wind speeds.

The spreading of a virus needs to be carefully modelled and simulated. Although the virus particles move in a multi-phase manner because they transmit in aerosols and droplets, they can also be simplified and modelled as a single-phase, massless gas (Rayegan, et al., 2022). As a result, we simulated all of the virus particles as a solvent in the air. The emission rate of virus particles from a patient in each case can be estimated to be at a constant rate of 42 quanta per hour for a light activity or speaking (Buonanno et al., 2020; Kurnitski et al., 2021). Consequently, we are able to simulate all of the cases in a steady-state flow. In addition, the source was modelled as the mouth of a patient

with dimensions of 0.05 x 0.10 m (Figure 3). The direction of the emission depends on the posture of the patient. The patients in the bedrooms lay down horizontally and therefore have an upward emission while that in the living room sits up vertically, hence emitting laterally.

Among many turbulence models available, Chen-Kim K- ϵ model was selected in this study because it can effectively imitate the situation of natural ventilation in and around buildings (Maragkogiannis et al., 2014). The calculation repeated 8,000 iterations in each case to reach satisfactory convergence. The residuals of mass in all of the cases passed the convergence criteria of being less than 0.1% (Srebric & Chen, 2002).

To ensure the accuracy of the results, we further perform a validation by comparing results from our CFD setups to those from a wind tunnel study (Ramponi & Blocken, 2012) as well as another CFD investigation that follows the former study (Sakiyama et al., 2021). We modelled a building that is the same size as the previous studies with dimensions of 10 x 10 x 8 m, which are similar in size to the detached house in this research (Figure 4). The building has a 4.6 x 1.8 m opening on the windward- and leeward-side walls, creating cross ventilation. The distances to the boundaries of the domain follow our setup rules. We simultaneously performed a grid independence study by comparing results from coarse, basic and fine grid setups with cell sizes of 0.5-0.7 m, 0.3-0.4 m and 0.2-0.3 m, respectively.

Figure 2

CFD Model Setups Showing the Dimensions of the Domain and Boundary Conditions.

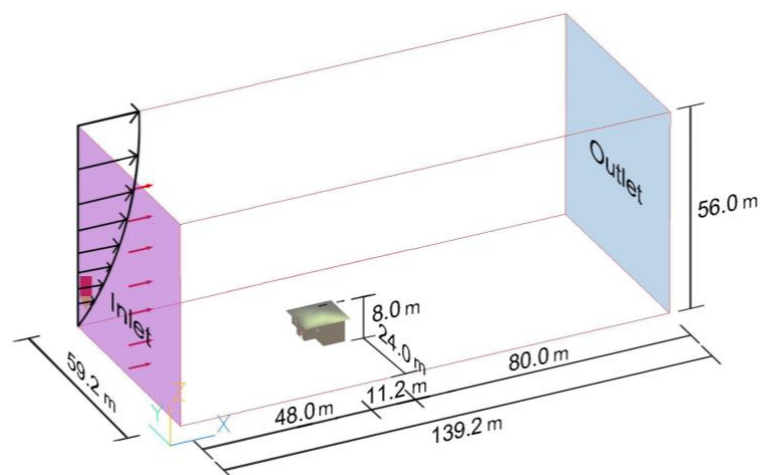


Figure 3

The Virus Emission of the Source in the CFD Models: (a) in the Bedrooms and (b) in the Living Room.

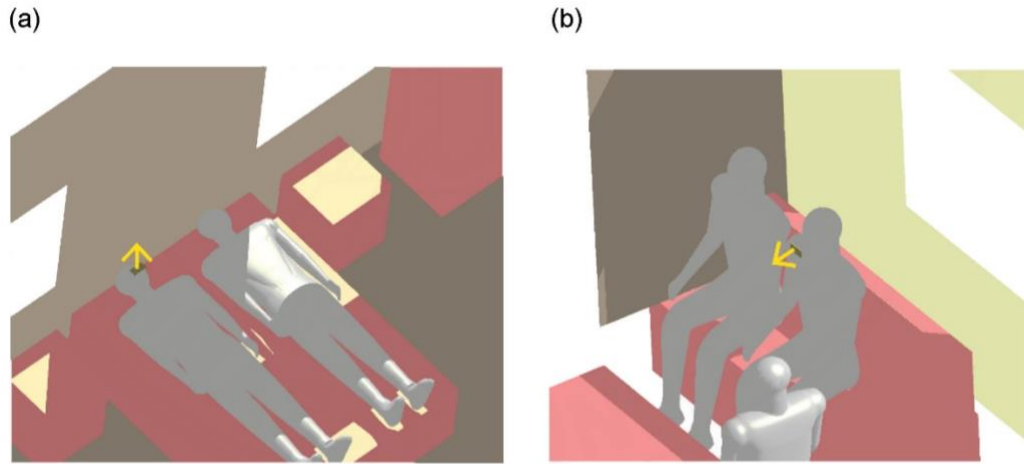
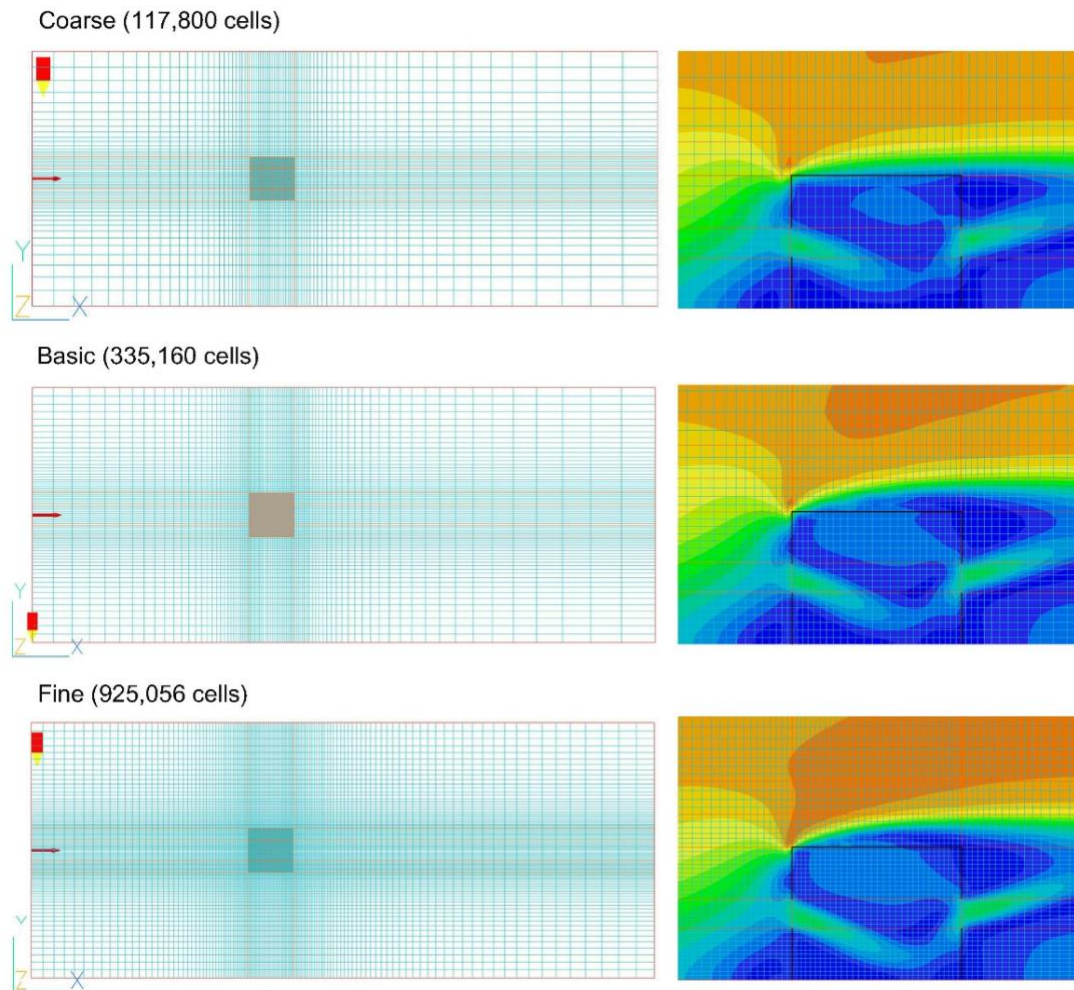


Figure 4

CFD Grid Setups and Results of the Validation Cases.



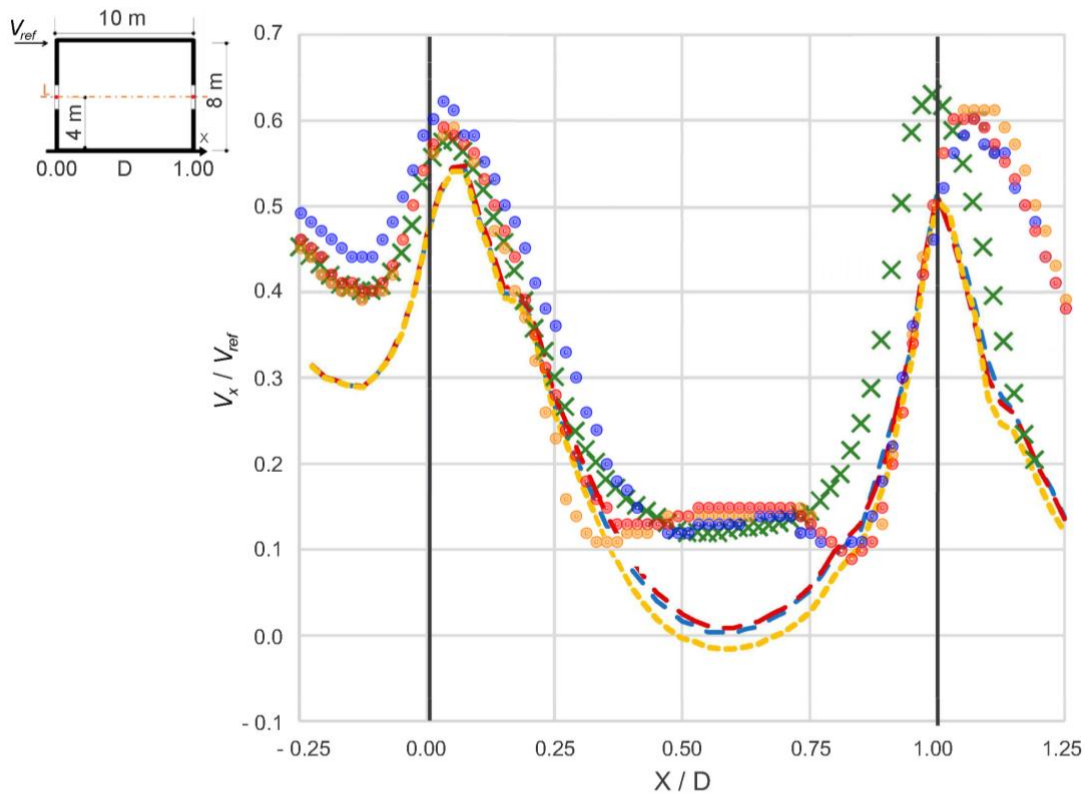
Air velocities from each of the grid setups were read from the same positions at 4 m above the ground at the centre of the opening along the cross section and demonstrated as a ratio to a reference velocity. The results were then compared to the previous studies (Figure 5). Root-mean-square error (RMSE) was recommended to be used as an indicator to

evaluate the compatibility of the results (van Druenen et al., 2019). The air velocity from our grid setup studies ($v1$) as compared to the previous studies ($v2$) gives the RMSE value as expressed in Equation (1).

$$RMSE = \sqrt{\frac{1}{n} \sum_{i=1}^n (v1_i - v2_i)^2} \quad (1)$$

Figure 5

Validation and Grid Independence Study Results Compared to the Results of 73 Values From Previous Studies.



- Coarse mesh
- Basic mesh
- Fine mesh
- × Ramponi & Blocken (2012)
- - - Sakiyama et al. (2021)

Ramponi & Blocken (2012)	RMSE
Coarse mesh (117,800 cells)	0.096
Basic mesh (335,160 cells)	0.096
Fine mesh (925,056 cells)	0.100

Sakiyama et al. (2021)	RMSE
Coarse mesh (117,800 cells)	0.135
Basic mesh (335,160 cells)	0.126
Fine mesh (925,056 cells)	0.124

Note. Adapted from “Using CFD to evaluate natural ventilation through a 3D parametric modeling approach,” by R. M. N. Sakiyama, J. Frick, T. Bejat, & H. Garrecht, 2021, *Energies*, 14(8), p.12 (<https://doi.org/10.3390/en14082197>). CC BY 4.0.

The comparative study demonstrates that our setups give a similar trend of results to the previous studies. The *RMSE* values of all of the cases are within the recommended range of 0.20 (van Druenen et al., 2019). The comparison also shows that the basic grid setup has similar *RMSE* values to the fine grid setup, meaning that it gives similar accuracy within shorter time. Therefore, we can use the basic grid setup in our study with confidence of its accuracy.

Evaluation methods

To evaluate the infection risk, we used air velocities at the inlet openings and virus concentration in each room from the CFD simulation. The air velocities were measured from 0.2 x 0.2 m meshes on vertical planes. The average air velocity from each case (v_a) was then multiplied by its opening area (A) to give a volumetric flow rate (Q) of the room. Virus concentration was measured at the height of 1.4 m above the floor, which is the breathing zone of a person in a sitting position. Measuring points are at the positions of the people for the calculation of personal infection risk and at every square metre of the space for the calculation of area infection risk. The Wells-Riley equation was then used to calculate the risk (Lim et al., 2010; Liu et al., 2022) as expressed in Equation (2).

$$P = 1 - e^{-C_i p t} \quad (2)$$

The infection risk (P) is a result of virus concentration at a position (C_i), the human breathing rate (p) and time of exposure in the space (t). In this research, we use the breathing rate of 0.00030556 m³/s (Adams, 1993; Binazzi, et al., 2006; Kurnitski et al., 2021) and estimate the time of exposure at 1 hour or 3,600 s in each space. We calculated the infection risk at each spot where occupants might be as a personal infection risk (P_p) ratio. The average risk of each room was also calculated from each square metre of the room as an area infection risk (P_a) ratio.

RESULTS

Master bedroom

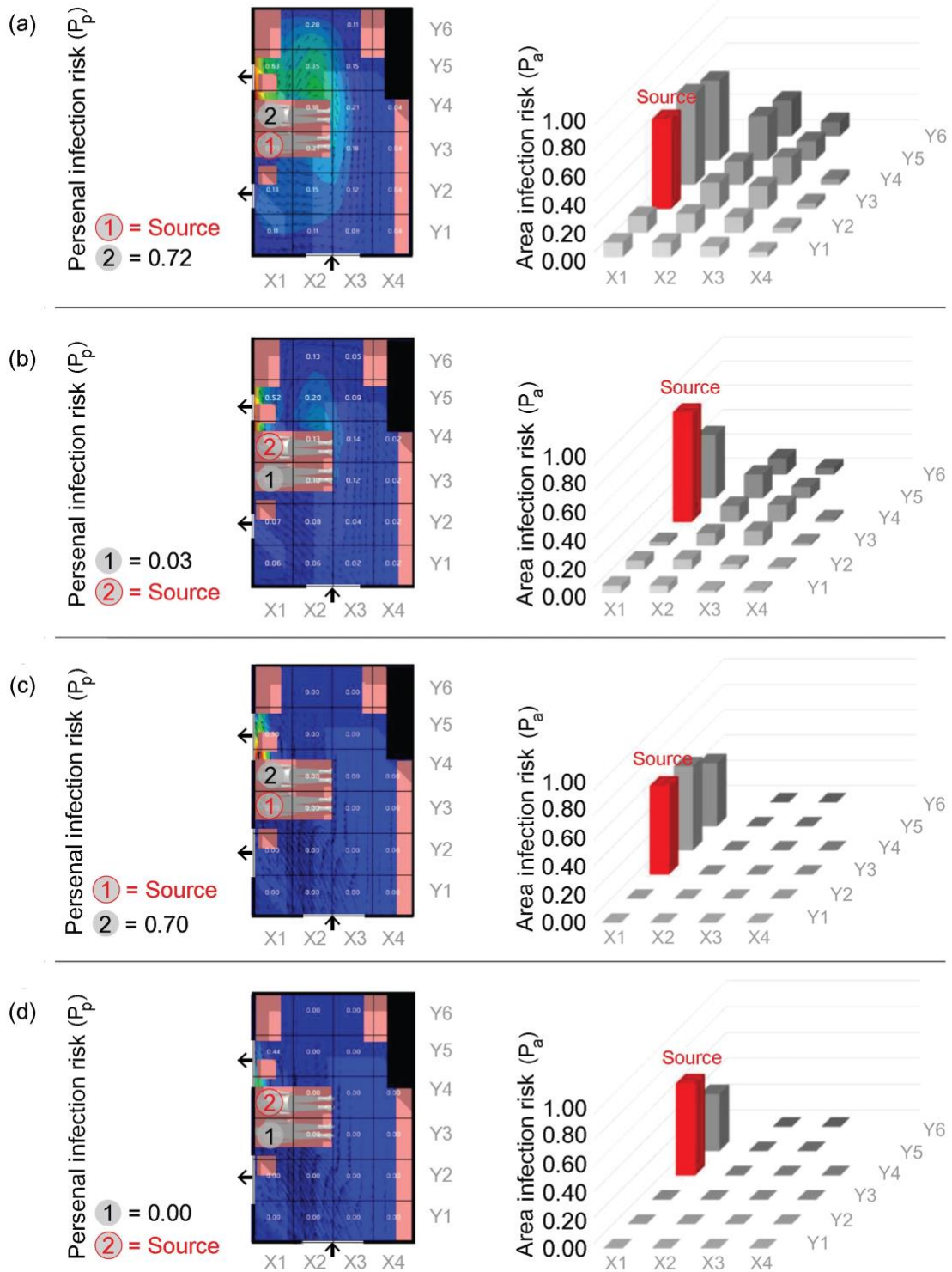
The CFD simulation of the master bedroom give the results that show the airflow behaviour and virus concentration as well as the calculation of infection risk (Figure 6). The volumetric flow rate of the cases of small openings and large openings can be calculated to be 2.10 and 4.40 m³/s, which give 102 ACH and 213 ACH, respectively.

The source in any of the master bedroom cases lies between two outlets while the air enters the room from the front of the house. This makes the virus particles leave the space only through the opening on the far end. If the patient is positioned at the windward side, the virus particles will move directly towards another person before exiting the room. This results in very high P_p ratios of 0.72 and 0.70 in small opening cases and large opening cases, respectively. On the other hand, if the patient is located at the leeward side, the virus particles will leave the space with little impact on another occupant. The P_p ratios are therefore much lower in the region of 0.03 and 0.00 in small opening cases and large opening cases, respectively. It can be seen that the opening size marginally affects the P_p ratios, although larger openings create a greater flow rate than the smaller openings by more than double.

The overall virus concentration in the room, evaluating through P_a , shows some impact from the opening size. In the small opening cases, recirculation occurs at the far end of the room (location Y5 and Y6) in a large area. This increases the accumulation of the virus particles as the P_a ratios are as high as 0.22 and 0.14 for the windward-side source and leeward-side source cases, respectively. Such numbers for the large opening cases are lower at 0.09 and 0.05 for the windward-side source and leeward-side source cases, respectively, because of the less stagnant area in the room.

Figure 6

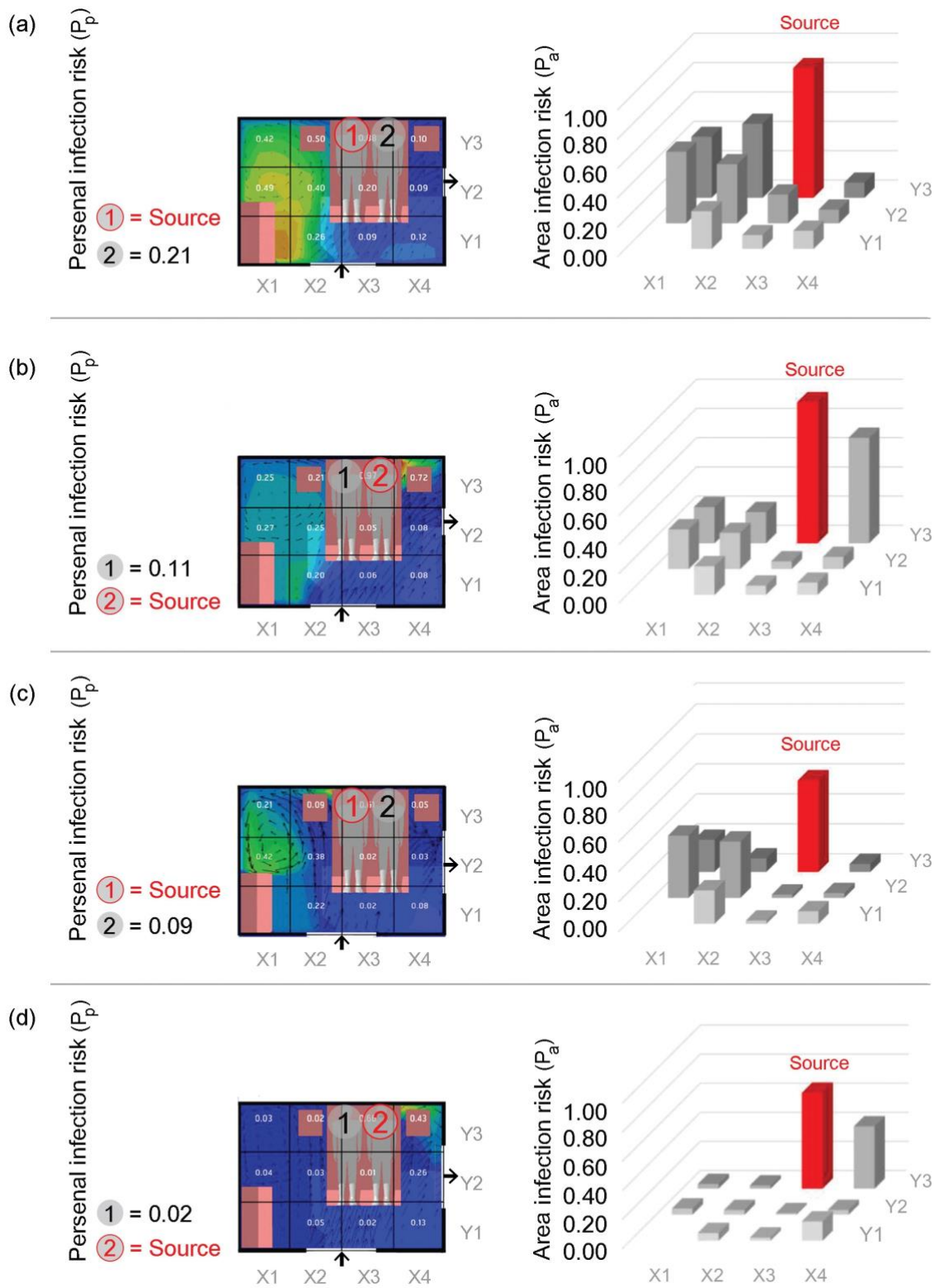
Simulation Results of the Master Bedroom Cases.



Note. (a) small openings and windward-side source, (b) small openings and leeward-side source, (c) large openings and windward-side source and (d) large openings and leeward-side source.

Figure 7

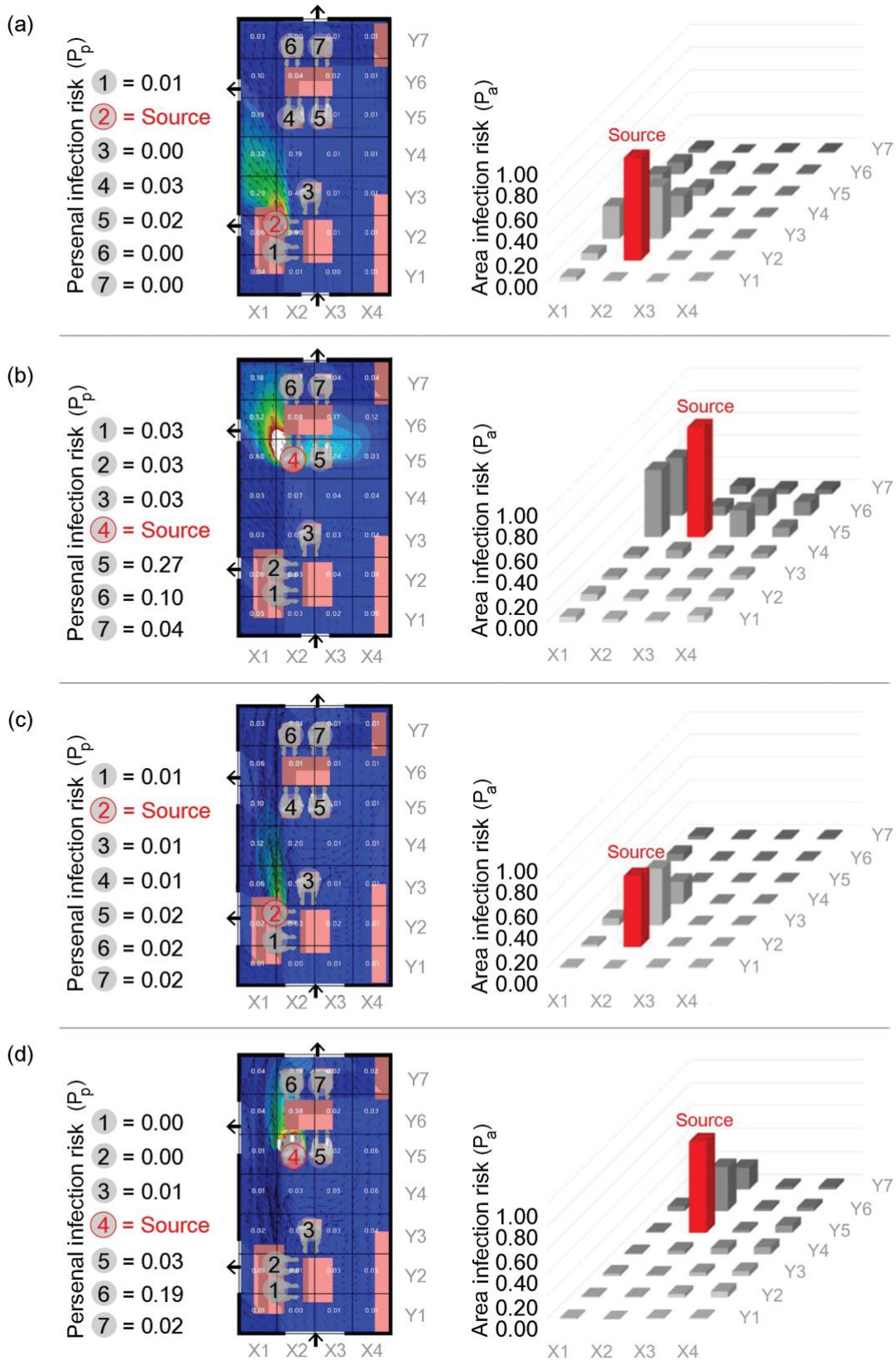
Simulation Results of the Bedroom Cases.



Note. (a) small openings and windward-side source, (b) small openings and leeward-side source, (c) large openings and windward-side source and (d) large openings and leeward-side source.

Figure 8

Simulation Results of the Living Room Cases.



Note. (a) small openings and windward-side source, (b) small openings and leeward-side source, (c) large openings and windward-side source and (d) large openings and leeward-side source.

Bedroom

We continued to study the results of airflow behavior, virus concentration and the calculation of infection risk from CFD simulation of the bedroom (Figure 7). In these cases, the volumetric flow rates of small opening and large opening cases can be calculated to be 1.28 and 2.13 m³/s, which give 128 ACH and 213 ACH, respectively.

The layout of the bedroom is different from the master bedroom and hence displays dissimilar airflow behaviour. Both occupants are located at the far end of the room, while the inlet opening is at the front of the house and the outlet opening is on the side. Such a configuration makes both occupants have a greater distance to the outlet opening than those in the master bedroom. The virus particles from the windward-side sources do not directly move to another occupant in the room but rather recirculate to another side of the room. The P_p ratios are therefore lower at 0.21 and 0.09 in small opening and large opening cases, respectively. In the cases where the patient is located at the leeward side, farther distances to the outlet allow the virus particles to stay in the room longer. The P_p ratios are therefore higher than those in the master bedroom at 0.11 and 0.02 in small opening and large opening cases, respectively.

There is a large recirculation area of air on the left side of the room (location X1 and X2) that affects the area infection risk. The air in the room has mixed more than the master bedroom. This results in higher P_a ratios. For small opening cases, the numbers are 0.29 and 0.26 for the windward-side source and leeward-side source cases, respectively. Although the values are lower in the large opening cases at 0.18 and 0.13 for the windward-side source and leeward-side source cases, respectively, they are higher than those of the master bedroom.

Living room

Airflow behavior, virus concentration and the calculation of infection risk of the living room are subsequently collected from the results of the CFD simulation (Figure 8). We calculated the volumetric flow rates of the small opening and

large opening cases to be at 2.26 and 5.09 m³/s, which give 92 ACH and 206 ACH, respectively.

In the living room, the functional space can clearly be divided into two smaller zones of living area and dining area. The air enters the room from the front of the house. Aside from an outlet opening at the end of the room, there are also two side openings acting as outlets. Virus particles can therefore leave the room through these side openings. In cases of the sources located at the windward side in the living area, the patients are positioned close to these side openings. The virus particles exit the room with little effect on other occupants, especially those in the dining area. As a result, the P_p ratios were found to be only at 0.03 and 0.02 for the small opening and large opening cases, respectively. On the other hand, if the sources are located at the leeward side in the dining area, the patients still affect other occupants sitting nearby in the same zone. This results in higher P_p ratios of 0.08 and 0.04 for the small opening and large opening cases, respectively.

The living room has openings on three sides, hence there is virtually little to no stagnant area. Compared to the cases of both master bedroom and bedroom, the P_a ratios are therefore lower. The risk numbers follow the size of the opening to a certain degree. In small opening cases, the values are 0.10 and 0.14 for the cases that have sources located at the windward side and leeward side, respectively. The numbers are lower in large opening cases at 0.07 and 0.07 for the cases with windward-side and leeward-side sources, respectively.

DISCUSSION

The results in general demonstrate that increasing the opening size will increase indoor air velocity and airflow rate thus reducing the overall airborne infection risk, which agrees with the previous study (Vita et al., 2023). In each of the three rooms in our study, the cases with larger openings show less infection risk ratios than those with smaller openings. However, the infection risk calculation in our study provides higher numbers than those in a previous study (Dai & Zhao, 2020), although our airflow rates are higher. This might result from the method of

our study that uses the Wells-Riley equation to estimate the infection risk at each spot in a space, which can be different from the study that assumes the air in the room is well mixed (Vita et al., 2023). A comparison of our results according to each of the influencing factors including opening size and location of the infect person is further discussed.

Opening size

The first influencing parameter of opening size is plotted with airborne infection risk both in terms of P_p ratio and P_a ratio (Figure 9). Each room differs in size. Therefore, we use opening-to-floor area ratio (OFR) instead of the opening area. It can be seen that the opening size affects both types of the infection risk ratios. Larger openings allow more volumetric flow rates, hence better diluting the air and affecting the overall infection risk ratios of a room. Increasing the OFR in the range of 0.03 to 0.28 will reduce the P_p ratios in the range of 0.01 to 0.12 while reducing the P_a ratios in a higher range of 0.03 to 0.13. The graphs of the P_a ratios in each room have more inclination than those of the P_p ratios. In addition, such effect applies only to the room of the same type and size. This is because each room has a different location of openings that creates a dissimilar area of stagnation. Each room also has a different position of the virus sources in relation to the openings and other occupants that causes alternated directions of air movement.

Location of the infected person

The accumulation of the virus particles relates to the direction of the indoor airflow. The location of the infected person in each case is therefore plotted with the airborne infection risk (Figure 10). It can be seen that the location of the source

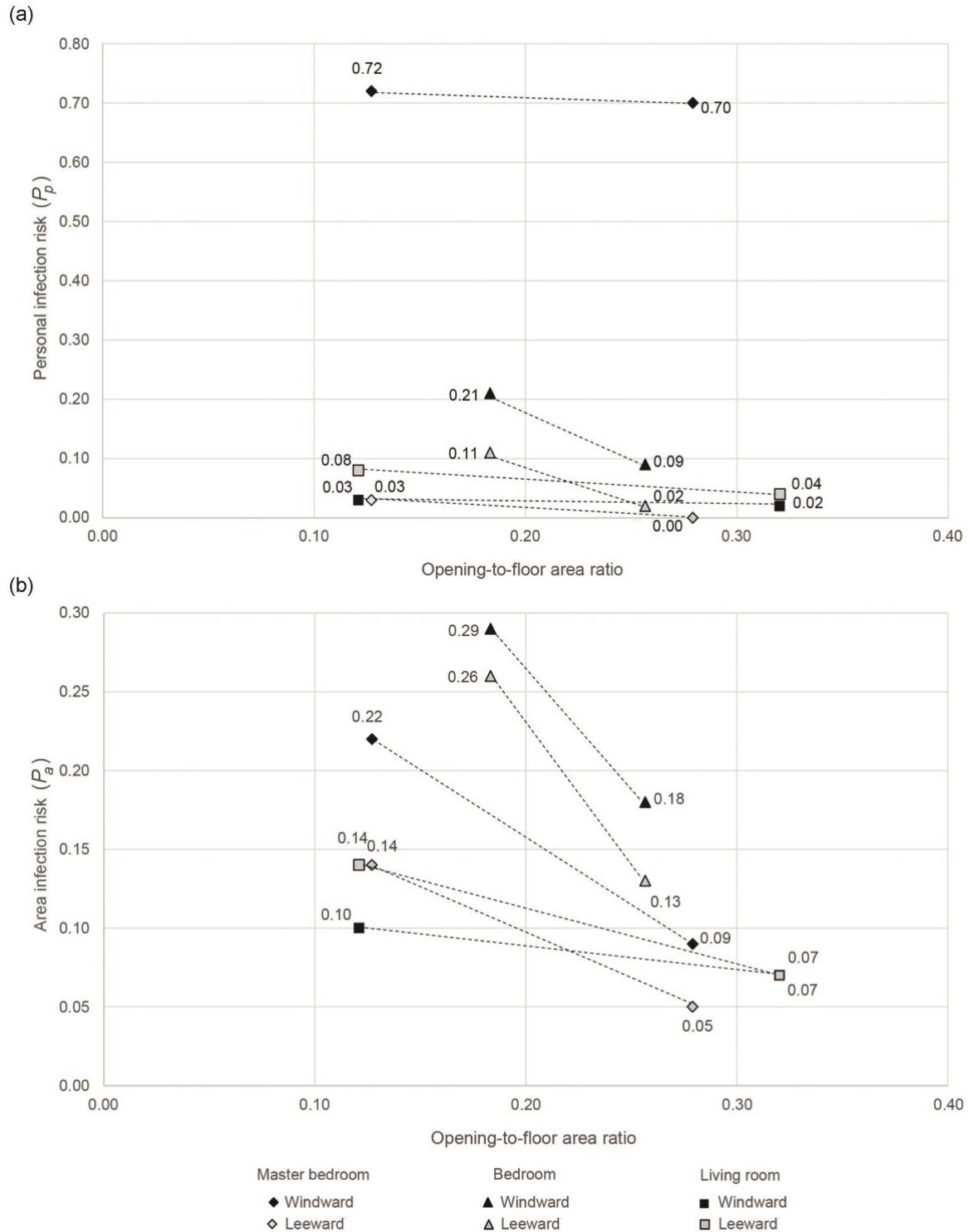
impacts the risk in various manners. The results show a significant effect on the P_p ratios in the master bedroom as the number differences of the windward-side cases and the leeward-side cases are as high as 0.69 to 0.70. This is because the locations of the infected person, another occupant and outlet opening all align in the same direction of air movement as well as having close proximity to one another. The differences in the bedroom are smaller in the range of 0.07 to 0.10 because the location of the source does not align in the same direction of air movement with the locations of another occupant and the outlet opening.

The P_a ratios have some influence from the location of the infected person in the master bedroom and bedroom albeit not as significant as the P_p ratios. The differences of the risk between the windward-side and leeward-side cases are similar in the range of 0.09 to 0.13 and 0.11 to 0.13 for the master bedroom and the bedroom, respectively. However, the P_a ratios also vary according to the efficiency of the airflow. Less efficient two-sided ventilation that occurs in the bedroom creates a recirculation area that accumulate virus particles to stay in the room longer than more efficient cross ventilation in the master bedroom and living room. The values in the bedroom (0.13 to 0.29) are therefore higher than those in the master bedroom (0.05 to 0.22) and living room (0.07 to 0.14).

In the living room, the P_p ratios display a reversed result because the room is divided into two zones and the air in windward-side case directly leaves the outlet while in the leeward-side case, meaning the air movement brings virus particles to the other occupants. The P_p ratios in the leeward-side cases are therefore higher than that in the windward-side cases in the range of 0.02 to 0.05. The P_a ratios in the living room also show the reversed result due to the same reason. The windward-side source creates more risk than the leeward-side source in the range of 0.00 to 0.04.

Figure 9

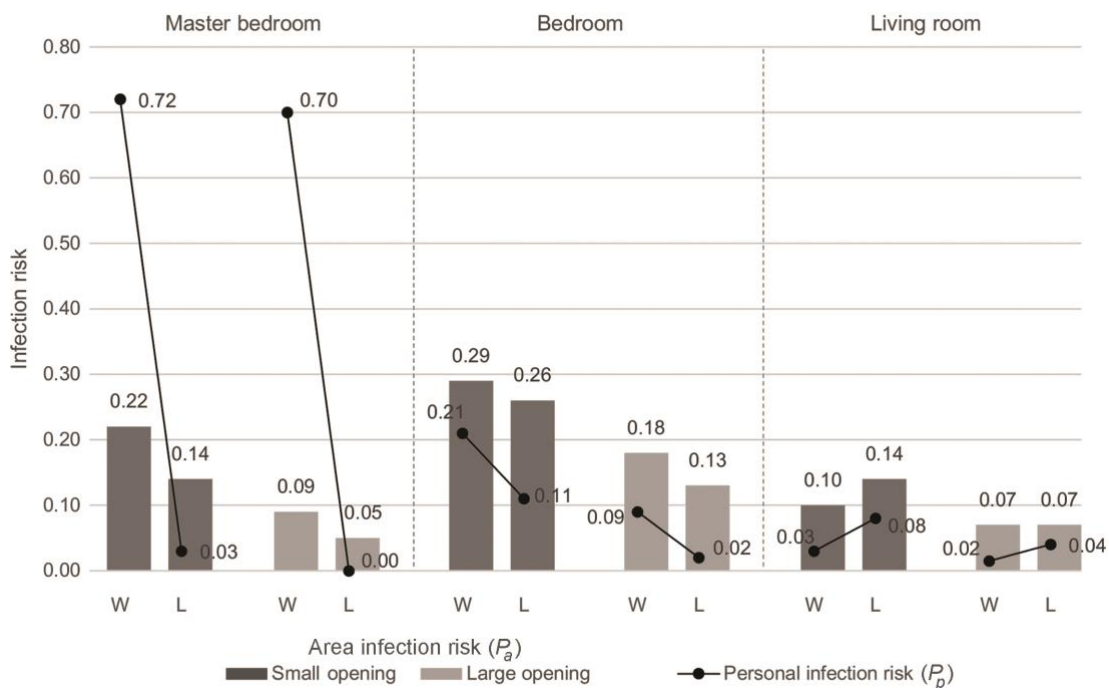
Graph Showing the Relationship of OFR and Airborne Infection Risk.



Note. (a) personal infection risk (P_p) and (b) area infection risk (P_a).

Figure 10

Graph Showing the Relationship of Location of the Infected Person (Windward side-W/Leeward side-L) and Airborne Infection Risk.



CONCLUSION

COVID-19 has caused huge global impact on humanity since its first outbreak in late 2019. The infection was found to be airborne; hence many efforts have been made with ventilation systems to better reduce the infection risk. However, the research gap for the study in residential buildings still remains, especially those including interior arrangement. As a result, this research studies a typical detached house, one of the most common building types in one of the most affected areas, Thailand.

A typical two-storied house was selected as a base case for this study. The master bedroom, bedroom and living room represent the spaces of our study with the variables of opening size and location of the infected person. A CFD program was used to assess the risk of the occupants from different setups. The virus particles were modeled in a simple single-phase, steady-state flow for the purpose of numerical efficiency. The setups were then validated with the results from previous studies to ensure the accuracy. We also performed the grid independency study and

found that the basic grid gives similar *RMSE* values to the fine grid when compared to the previous studies and should be further used in this study. The CFD results were subsequently interpreted to airborne infection risks as P_p ratio and P_a ratio using the Wells-Riley equation.

Results from the 12 CFD cases were reported. In the master bedroom, the windward-side sources create very high P_p ratios to the occupants while the opposite leeward-side sources generate very low rates because of the direct alignment of the sources, the occupants and the outlets. The P_a ratios follow the opening size: larger openings create lower risks. In the bedroom, the location of the infected person and the other occupant in relation to the outlet openings are farther than the master bedroom. The P_p ratio discrepancies between the windward-side and leeward-side sources are therefore lower. The P_a ratios in these cases also follow the opening size. However, all of the risks in the living room show different trends because the room has two zones and the location of the infected person in each zone affects the other occupants differently. There are less stagnant areas in the living room

which create lower P_a ratios than the other rooms.

The results were further compared following the two influencing variables. Opening size affects more on the P_a ratios than the P_p ratios. A larger opening creates less risk in any pairing cases of the same room type while cross ventilation creates less risk than two-sided ventilation. The location of the infected person, however, impacts more on the P_p ratios than the P_a ratios. It significantly varies the trend of the risk according to other factors including the location of the other occupants and the openings, especially on the outlet side. Further investigation of more relationships among these parameters could be the subject of future studies along with the effect of opening in more varied sizes and the prevailing wind from other directions.

In practice, this research implies that the design should focus beyond general guidelines that give certain airflow rates for a space. In naturally ventilated spaces, larger opening sizes and more effective ventilation types create lower overall infection risk. However, although the ACH values are much higher than those given in the standards, some local areas still face high ratios of infection risk. Concentration should also be placed on the direction of the disease dispersion from the infected person. Locating the infected person in the areas closed to the outlet opening would reduce the infection risk of other occupants sharing the same space.

DISCLOSURE AND ACKNOWLEDGEMENT

The authors thank the support on Thammasat Research Unit in Architecture for Sustainable Living and Environment. The authors report there are no competing interests to declare.

REFERENCES

- Adams, W. C. (1993). *Measurement of breathing rate and volume in routinely performed daily activities-Final Report Contract (1993) A033–A205*. United State Environmental Protection Agency.
https://hero.epa.gov/hero/index.cfm/reference/details/reference_id/77086
- Alraouf, A. A. (2021). The new normal or the forgotten normal: Contesting COVID-19 impact on contemporary architecture and urbanism. *Archnet-IJAR*, 15(1), 167–188.
<https://doi.org/10.1108/ARCH-10-2020-0249>
- Allen, J. G., & Ibrahim, A. M. (2021). Indoor air changes and potential implications for SARS-CoV-2 transmission. *Journal of the American Medical Association*, 325(20), 2112–2113.
<https://doi:10.1001/jama.2021.5053>
- American Society of Heating, Refrigerating and Air-Conditioning Engineers. (2021). *Guidance for COVID-19 risk reduction in residential buildings*.
<https://www.ashrae.org/technical-resources/guidance-for-covid-mitigation-in-residential-buildings#isolation>
- Atkinson, J., Chartier, Y., Pessoa-Silva, C. L., Jensen, P. Li, Y., & Seto, W. H. (2009). *Natural ventilation for infection control in healthcare settings*. World Health Organization.
<https://www.who.int/publications/i/item/9789241547857>
- Bangkok Post. (2022, January 27). *Covid to be declared endemic by year's end in Thailand*.
<https://www.bangkokpost.com/thailand/general/2254503/covid-to-be-declared-endemic-by-years-end-in-thailand>
- Bettaieb, D. M., & Alsabban, R. (2021). Emerging living styles post-COVID-19: Housing flexibility as a fundamental requirement for apartments in Jeddah. *Archnet-IJAR*, 15(1), 28–50.
<https://doi.org/10.1108/ARCH-07-2020-0144>

Binazzi, B., Lanini, B., Bianchi, R., Romagnoli, I., Nerini, M., Gigliotti, F., Duranti, R., Milic-Emili, J., & Scano, G. (2006). Breathing pattern and kinematics in normal subjects during speech, singing and loud whispering. *Acta Physiologica*, 186(3), 233–246. <https://doi.org/10.1111/j.1748-1716.2006.01529.x>

Buonanno, G., Morawska, L., & Stabile, L. (2020). Quantitative assessment of the risk of airborne transmission of SARS-CoV-2 infection: Prospective and retrospective applications. *Environment International*, 145, Article 106112. <https://doi.org/10.1016/j.envint.2020.106112>

Concentration, Heat and Momentum Limited. (2021). *Phoenixs 2021*. https://www.cham.co.uk/_docs/pdfs/phoenixs_docs/phoenixs_2021.pdf

Cheng, P., Chen, W., Xiao, S., Xue, F., Wang, Q., Chan, P. W., You, R., Lin, Z., Niu, J., & Li, Y. (2022). Probable cross-corridor transmission of SARS-CoV-2 due to cross airflows and its control. *Building and Environment*, 218, Article 109127. <https://doi.org/10.1016/j.buildenv.2022.109137>

Cheung, T., Li, J., Goh, J., Sekhar, C., Cheong, D., & Tham, K. W. (2022). Evaluation of aerosol transmission risk during home quarantine under different operating scenarios: A pilot study. *Building and Environment*, 225, Article 109640. <https://doi.org/10.1016/j.buildenv.2022.109640>

Dai, H., & Zhao, B. (2020). Association of the infection probability of COVID-19 with ventilation rates in confined spaces. *Building Simulation*, 13, 1321–1327. <https://doi.org/10.1007/s12273-020-0703-5>

Dai, Y., Xu, D., Wang, H., & Zhang, F. (2023). CFD Simulations of ventilation and interunit dispersion in dormitory complex: A case study of epidemic outbreak in Shanghai. *International Journal of Environmental Research and Public Health*, 20(5), Article 4603. <https://doi.org/10.3390/ijerph20054603>

Inprom, N., & Jareemit, D. (2021). Efficient envelope designs to maximize cooling energy savings in housing complexes in Bangkok neighborhoods. *Nakhara: Journal of Environmental Design and Planning*, 20(1), Article 103. <https://doi.org/10.54028/NJ202120103>

Inthisorn, P., & Puttanapong, N. (2022). Associations between mobility indices and the COVID-19 pandemic in Thailand. *Nakhara: Journal of Environmental Design and Planning*, 21(2), Article 215. <https://doi.org/10.54028/NJ202221215>

Kurnitski, J. (2020). Ventilation rate and room size effects on infection risk of COVID-19. *The REHVA European HVAC Journal*, 57(5), 26–31. <https://www.rehva.eu/rehva-journal/chapter/ventilation-rate-and-room-size-effects-on-infection-risk-of-covid-19>

Kurnitski, J., Kiil, M., Wargocki, P., Boerstra, A., Seppänen, O., Olesen, B., & Morawska, L. (2021). Respiratory infection risk-based ventilation design method. *Building and Environment*, 206, Article 108387. <https://doi.org/10.1016/j.buildenv.2021.108387>

Li, X., Lester, D., Rosengarten, G., Aboltins, C., Patel, M., & Cole, I. (2023). A spatiotemporally resolved infection risk model for airborne transmission of COVID-19 variants in indoor spaces. *Science of the Total Environment*, 812, Article 152592. <https://doi.org/10.1016/j.scitotenv.2021.152592>

Li, Y., Qian, H., Hang, J., Chen, X., Cheng, P., Ling, H., Wang, S., Liang, P., Li, J., Xiao, S., Wei, J., Liu, L., Cowling, B. J., & Kang, M. (2021). Probable airborne transmission of SARS-CoV-2 in a poorly ventilated restaurant. *Building and Environment*, 196, Article 107788. <https://doi.org/10.1016/j.buildenv.2021.107788>

Lim, T., Cho, J., & Kim, B. S. (2010). The predictions of infection risk of indoor airborne transmission of diseases in high-rise hospitals: Tracer gas simulation. *Energy and Buildings*, 42(8), 1172–1181. <https://doi.org/10.1016/j.enbuild.2010.02.008>

- Liu, M., Liu, J., Cao, Q., Li, X., Liu, S., Ji, S., Lin, C., Wei, D., Shen, X., Long, Z., & Chen, Q. (2022). Evaluation of different air distribution systems in a commercial airliner cabin in terms of comfort and COVID-19 infection risk. *Building and Environment*, 208, Article 108590. <https://doi.org/10.1016/j.buildenv.2021.108590>
- Maragkogiannis, K., Kolokotsa, D., Maravelakis, E., & Konstantaras, A. (2014). Combining terrestrial laser scanning and computational fluid dynamics for the study of the urban thermal environment. *Sustainable Cities and Society*, 13, 207–216. <https://doi.org/10.1016/j.scs.2013.12.002>
- Mediastika, C. E., Kristanto, L., Anggono, J., Suhedi, F., & Purwaningsih, H. (2018). Open windows for natural airflow and environmental noise reduction. *Architectural Science Review*, 61(5), 338–348. <https://doi.org/10.1080/00038628.2018.1502151>
- Mohamadi, F., & Fazeli, A. (2022). A review on applications of CFD modeling in COVID-19 pandemic. *Archives of Computational Methods in Engineering*, 29, 3567–3586. <https://doi.org/10.1007/s11831-021-09706-3>
- O'Donovan, A., & O'Sullivan, P. D. (2023). The impact of retrofitted ventilation approaches on long-range airborne infection risk for lecture room environments: Design stage methodology and application. *Journal of Building Engineering*, 68, Article 106044. <https://doi.org/10.1016/j.jobe.2023.106044>
- Panraluk, C., & Sreshtaputra, A. (2020). Development of guidelines for enhancement of thermal comfort and energy efficiency during winter for Thailand's senior centers using surveys and computer simulation. *Nakhara: Journal of Environmental Design and Planning*, 19, 79–96. <https://doi.org/10.54028/NJ2020197996>
- Park, S., Choi, Y., Song, D., & Kim, E. (2021). Natural ventilation strategy and related issues to prevent coronavirus disease 2019 (COVID-19) airborne transmission in a school building. *Science of the Total Environment*, 789, Article 147764. <https://doi.org/10.1016/j.scitotenv.2021.147764>
- Peters, T., & Halleran, A. (2021). How our homes impact our health: Using a COVID-19 informed approach to examine urban apartment housing. *Archnet-IJAR*, 15(1), 10–27. <https://doi.org/10.1108/ARCH-08-2020-0159>
- Ramponi, R., & Blocken, B. (2012). CFD simulation of cross-ventilation for a generic isolated building: Impact of computational parameters. *Building and Environment*, 53, 34–48. <https://doi.org/10.1016/j.buildenv.2012.01.004>
- Rayegan, S., Shu, C., Berquist, J., Joen, J., Zhou, L., Wang, L., Mbareche, H., Tardif, P., & Ge, H. (2022). A review on indoor airborne transmission of COVID-19— modelling and mitigation approaches. *Journal of Building Engineering*, 64, Article 105599. <https://doi.org/10.1016/j.jobe.2022.105599>
- Sakiyama, R. M. N., Frick, J., Bejat, T., & Garrecht, H. (2021). Using CFD to evaluate natural ventilation through a 3D parametric modeling approach. *Energies*, 14(8), Article 2197. <https://doi.org/10.3390/en14082197>
- Salama, A. M. (2020). Coronavirus questions that will not go away: Interrogating urban and sociospatial implications of COVID-19 measures. *Emerald Open Research*, 2020, 1(5), 1–17. <https://doi.org/10.35241/emeraldopenres.13561.1>
- Schoen, L. J. (2020). Guidance for building operations during the COVID-19 pandemic. *ASHRAE Journal*, 62(5), 72–74. https://www.ashrae.org/file%20library/technical%20resources/ashrae%20journal/2020journaldocuments/72-74_ieq_schoen.pdf

Srebric, J., & Chen, Q. (2002). An example of verification, validation, and reporting of indoor environment CFD analyses. *ASHRAE Transactions*, 108(2), 185–194.
<https://engineering.purdue.edu/~yanchen/paper/2002-9.pdf>

Tantasavasdi, C., Sreshthaputra, A., Suwanchaiskul, A., & Pichaisak, M. (2009). Predicting airflow in naturally-ventilated generic houses. *Journal of Architectural/Planning Research and Studies*, 6(1), 31–46.
<https://doi.org/10.56261/jars.v6i1.168778>

van Druenen, T., van Hooff, T., Montazeri, H., & Blocken, B. (2019). CFD evaluation of building geometry modifications to reduce pedestrian-level wind Speed. *Building and Environment*, 163, Article 106293.
<https://doi.org/10.1016/j.buildenv.2019.106293>

Vita, G., Woolf, D., Avery-Hickmott, T., & Rowsell, R. (2023). A CFD-based framework to assess airborne infection risk in buildings. *Building and environment*, 233, Article 110099.
<https://doi.org/10.1016/j.buildenv.2023.110099>

World Health Organization. (2021). *Coronavirus disease (COVID-19): Ventilation and air conditioning*. <https://www.who.int/news-room/questions-and-answers/item/coronavirus-disease-covid-19-ventilation-and-air-conditioning>

World Health Organization. (2023). *WHO Coronavirus (COVID-19) dashboard*. <https://covid19.who.int/>

World Health Organization Thailand. (2023). *WHO Thailand weekly situation update No. 259*. <https://www.who.int/thailand/news/detail/15-03-2023-the-situation-report-on-covid19>

Zhu, S., Jenkins, S., Addo, K., Heidarinejad, M., Romo, S. A., Layne, A., Ehizibolo, J., Dalgo, D., Mattise, N. W., Hong, F., Adenaiye, O. O., de Mesquita, J., Albert, B. J., Washington-Lewis, R., German, J., Tai, S., Youssefi, S., Milton, D. K., & Srebric, J. (2020). Ventilation and laboratory confirmed acute respiratory infection (ARI) rates in college residence halls in College Park, Maryland. *Environment International*, 137, Article 105537.
<https://doi.org/10.1016/j.envint.2020.105537>